



## Rock-forming mechanism of Qingshanjiao intrusion in Dongguashan copper (gold) deposit, Tongling area, Anhui province, China

Zhong-fa LIU<sup>1,2</sup>, Yong-jun SHAO<sup>1,2</sup>, Han-tao WEI<sup>1,2</sup>, Cheng WANG<sup>1,2</sup>

1. Key Laboratory of Metallogenic Prediction of Nonferrous Metals and Geological Environment Monitor, Ministry of Education, Central South University, Changsha 410083, China;
2. School of Geoscience and InfoPhysics, Central South University, Changsha 410083, China

Received 9 July 2015; accepted 18 May 2016

**Abstract:** Dongguashan deposit is a large porphyry-skarn copper (gold) deposit in Tongling ore district. The Qingshanjiao intermediate acid intrusion of Yanshanian had a direct genetic relationship with mineralization. The magma origin, rock-forming dynamic background and rock-forming process were studied, and the rock-forming mechanism of Qingshanjiao intrusion was discussed, based on geological characteristics, detailed observation of petrography and systematic investigation of petrochemistry, trace elements and REE geochemistry characteristics of Qingshanjiao intrusion. The results show that Qingshanjiao rock body belongs to high-K calc-alkaline series with higher LREE elements, Th, Rb and Sr abundance, but depleted in HREE elements, Ba, Nb and Ta. The primary magma originated from the mantle-crust mixtures which were caused by basaltic magma of mantle mixing with syenite magma of partial melting of the lower crust, and the formation environment of Qingshanjiao intrusion was emplaced in the transitional environment from compression to extension. The Harker diagram and hybrid structures of plagioclase and potassium feldspar indicate that the fractional crystallization occurred in the process of magmatic evolution. The petrochemistry, trace elements and REE geochemistry characteristics indicate that the magma was contaminated by crustal material during the rock-forming. These results suggested that the Qingshanjiao intrusion was formed by fractional crystallization and assimilation and hybridization of mantle-crust magma in the transitional environment from compression to extensional.

**Key words:** Qingshanjiao intrusion; geological and geochemical characteristics; rock-forming and geodynamic setting; magma derivation; rock-forming; Dongguashan copper (gold) deposit

### 1 Introduction

Dongguashan copper (gold) deposit is one of the important parts of the Tongling ore district. It is located in the northeast margin of the Yangtze block, and belongs to the Middle-Lower Yangtze River Valley Metallogenic Belt in Eastern China (Fig. 1), which is a part of Fanchang—Guichi fault-fold belt of the Lower Yangtze syncline [1]. It is also a part of the northeast section of the Qingshan anticline which is secondary structure of the Datong—Shun'an multiple syncline. Since Mesozoic, the Middle-Lower Yangtze area, including Tongling ore district entered into an active phase of tectonic movement. The strong tectonic movement of Yanshanian caused intensive intermediary to acidic magmatic movement. Intermediary to acidic magmatic rocks are

extensively outcropped, associated with a series of Cu, Fe, Au, Pb and Zn metallogenic activities.

The magmatism process and genesis of magmatic rock have been the focus of geological study. Previous studies were conducted on the intrusive rocks within Shizishan orefield in terms of geochemical features of the intrusive rocks, rock-forming age and genesis of rock [2–9], and it is suggested that the Yanshanian intermediate-acid intrusions are closely associated with the mineralization. The results of previous studies in this area provide rich information of rock geochemistry and geochronology. Because of the different research methods and perspective, there is still controversy on the magma origin. Systematic studies focused on the genesis mechanism of Qingshanjiao intrusion are seldom reported. The Qingshanjiao intrusion is closely associated with Dongguashan copper (gold) deposit,

especially the plutonic porphyry orebody. Therefore, it is essential to study the rock-forming mechanism in terms of the source of magma, rock-forming environment, and the rock-forming process, based on the studies of petrography, petrogeochemistry, geochemistry of trace elements and REE for the Qingshanjiao intrusion. The study will have significant influence on the study of rock and ore-forming processes, source of ore-forming materials, source of metallogenic fluid as well as the genesis of the deposit. It also provides an example for studying the genetic mechanism and tectonic setting of Mesozoic intermediate-acid intrusive rock bodies.

## 2 Geological and lithological features of intrusion

Qingshanjiao intrusion is located in Shizishan orefield in Tongling ore district (Fig. 2), distributing in the southeastern part of Line 34 to Line 54 of Dongguashan deposit. The outcrop is less than 100 m. The width is 150 m at  $-400$  m elevation, and more than 300 m at  $-600$  m elevation. The intrusion is narrow at the top and wide at the bottom in the form of a dyke. The rock strikes NE and dips SE are almost vertical, due to influences from the NE-striking structure. Small apophysis is well developed around the intrusion, and stretches into the wall rock along bedding in the manner of tree branches. Close to the intrusion, both width of the ore-body and mineral concentration increase. The porphyry close to the intrusion is well mineralized (as seen from intersections by the boreholes ZK483, ZK5415, ZK415, ZK5417). Trace element analysis (Dongguashan copper deposit internal data) and S, Pb isotope [10] indicate that Qingshanjiao intrusion is closely related to the mineralization. The intrusion is

dominantly composed of quartz monzodiorite and porphyraceous granodiorite.

WU et al [11] and TANG et al [1] reported Ar–Ar isotopic dating of the Dongguashan magmatic rocks of  $(135.8 \pm 1.1)$  Ma and 135.8 Ma. XU et al [12] conducted whole rock Rb–Sr isotopic dating of Qingshanjiao intrusion of  $(135.6 \pm 1.4)$  Ma. LU [13] and XU et al [14] reported zircon SHRIMP U–Pb dating of the Dongguashan quartz monzodiorite of  $(136.0 \pm 2.0)$  Ma and  $(135.5 \pm 2.2)$  Ma, respectively. All the above results indicate that the magmatic activities of the area mainly occur at around 135 Ma, and the magmatic rocks belong to Yanshanian magmatic rock. Mineralization which is related to the intrusion mainly includes skarn-type mineralization and porphyry-type mineralization. The skarn minerals are mainly garnet, diopside, forsterite, humite, tremolite, serpentine, epidote and actinolite.

Qingshanjiao unaltered intrusion is grey, grayish-white, medium-coarse granular texture, porphyraceous texture and hybrid texture (Figs. 3(a) and (b)). The primary minerals are mainly plagioclase (45%–50%), potash feldspar (10%–15%), quartz (15%–20%) and hornblende (10%), secondly for microcline, biotite, epidote and chlorite. Accessory minerals are pyrite, chalcopyrite, apatite and sphene, which fill the interval space between other minerals with allotromorphic granular texture or replace earlier minerals.

The plagioclase of the Qingshanjiao intrusion is dominantly andesine, with columnar or tabular crystal form. Polysynthetic twin crystals are commonly seen. Zonal texture can be universally observed in plagioclase (Fig. 3(c)). Hydrothermal alterations include sericitization and carbonatization (Fig. 3(e)). Early plagioclase is dissolved and replaced by later minerals

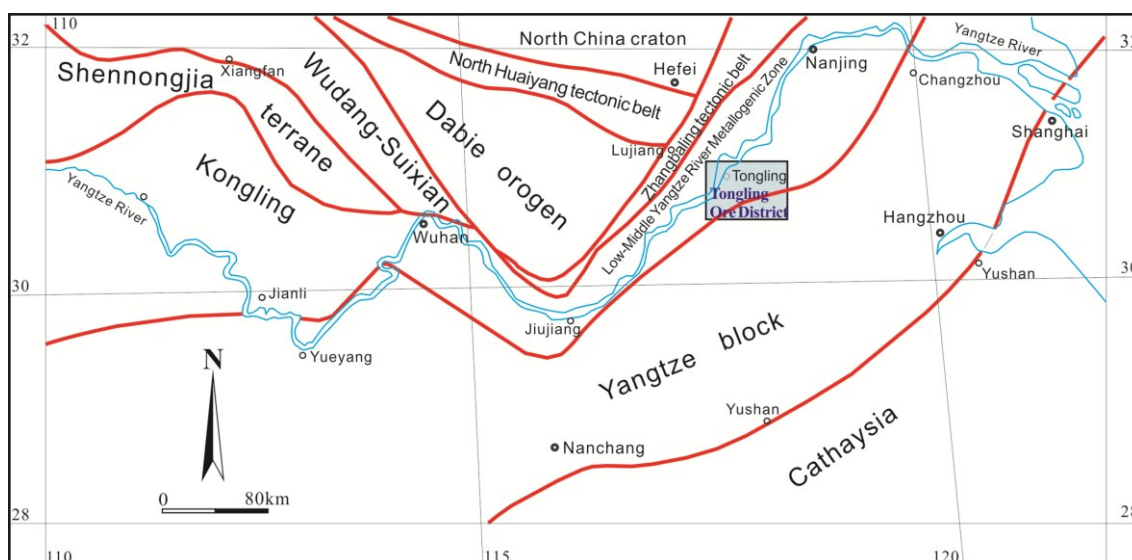
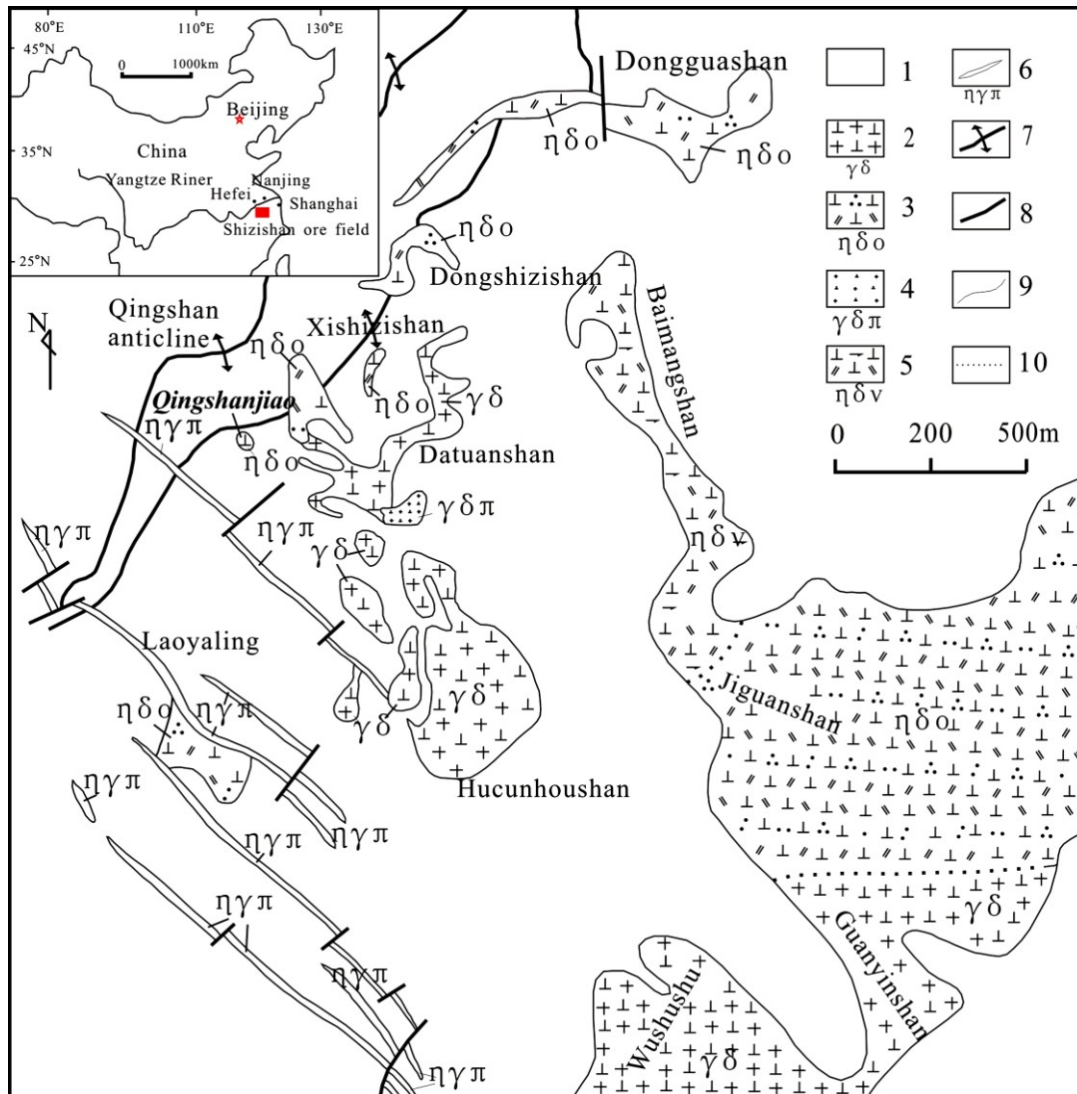


Fig. 1 Location of Tongling ore district in Yangtze River belt



**Fig. 2** Distribution map of intrusions in Shizishan orefield (Modified from XU et al [14]): 1—Middle-upper triassic limestone, sandstone; 2—Grano-diorite; 3—Quarz monzonite diorite; 4—Grano-diorite-porphry; 5—Pyroxene monzonite diorite; 6—Monzonite grano-porphry; 7—Anticline axis; 8—Fault; 9—Geological boundary; 10—Inferred boundary

(Fig. 3(f)). The potash feldspar is mainly subhedral-allotromorphic columnar crystal which is typical characteristics of potash feldspar. Carlsbad twin crystals are also observed. The potash feldspar is partly replaced by microcline, and shows potash feldspar pseudomorph (Fig. 3(g)). The hornblende is the major dark mineral in this area, with subhedral-allotromorphic crystal and partly chloritization (Fig. 3(h)).

### 3 Geochemical features

#### 3.1 Sampling and testing methods

The intrusion testing samples were collected from Qingshanjiao intrusion of exploration Line 59 and Line 66 at -850 m underground adits, part of the boreholes. The rocks were fresh and un-altered (no mineralization and without transforming other minerals). Test method is

described as follows. 1) Trace elements: first, the sample was dissolved with HNO<sub>3</sub>-HClO<sub>4</sub>-HF-HCl solution, after the sample was evaporated, the dissolution and constant volume were finished by using dilute hydrochloric acid. At last, the results were tested by inductively coupled plasma spectrometer (ICP-AES). 2) Rare earth elements: the sample that was well-mixed with LiBO<sub>2</sub>/Li<sub>2</sub>B<sub>4</sub>O<sub>7</sub> was melted in furnace at above 1025 °C, after the molten cooling, the constant volume was finished by using HNO<sub>3</sub>-HClO<sub>4</sub>-HF-HCl solution. At last, the results were tested by inductively coupled plasma massspectrometry (ICP-MS). 3) Major elements: the sample was melted with lithium nitrate, regarding the molten material into glass sheet. At last, the results were tested by X-ray fluorescence spectrometer (XRF). All of the tests were conducted by Aoshi Laboratory, Guangzhou, China.

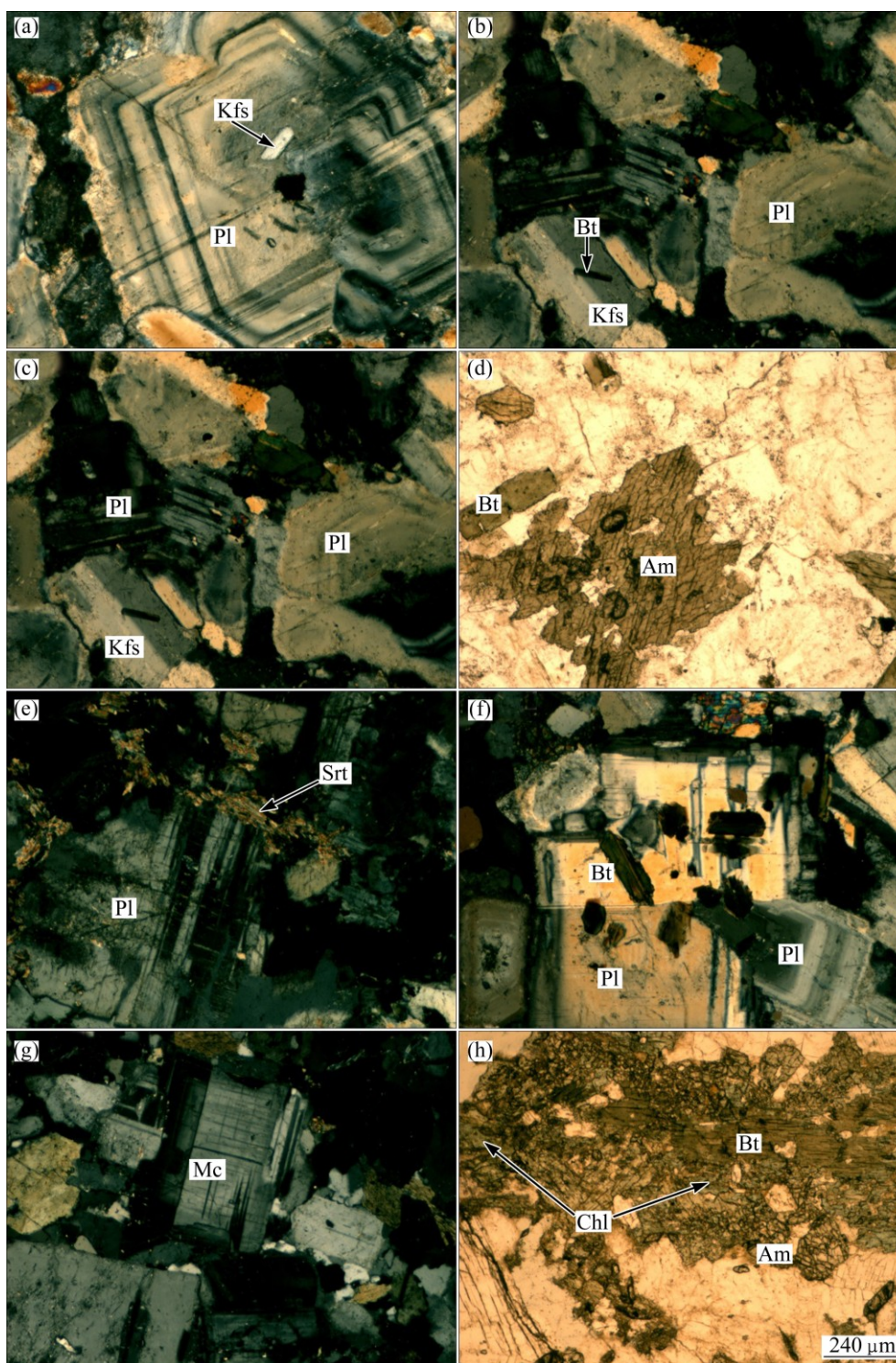


**Fig. 3** Microscopic features of Qingshanjiao intrusion: (a) Plagioclase zoning texture and poikilitic texture (+); (b) K-feldspar poikilitic texture (+); (c) Hypidiomorphic–allotriomorphic texture (+); (d) Two sets of hornblendes with clear oblique cleavage, replaced by later epidote (-); (e) Plagioclase with clear twinning striation, with alterations including sericitization on the surface (+); (f) Plagioclase with clear zoning features, replaced by biotite (-); (g) Microcline with tartan twinning, replacing K-feldspar and showing K-feldspar pseudomorph (+); (h) Hornblende and biotite with chloritization (-) (Pl—Plagioclase; Kfs—K-feldspar; Bt—Biotite; Am—Amphibole; Srt—Sericite; Chl—Chlorite; Mc—Microcline; (+)—Cross-polarized light; (-)—Catoptric light)

### 3.2 Petrochemical characteristics

The studies of petrochemistry of Qingshanjiao intrusion (Table 1) show that the content of  $\text{SiO}_2$  is

56.83%–62.59%, averaging 59.10%, which is between the average value of diorite (57.39%) and quartz diorite (60.51%) (Li [15], the same below). Total alkali

**Table 1** Major elements contents and characteristic values of Qingshanjiao intrusion (mass fraction, %)

Parameter	TS003-1	DK001-4	DK004-3	DK004-4	DK004-5	DK005-1	DGS8-11	DGS3-11	DGS8-8	ZK-51	Total	Average value
w(SiO <sub>2</sub> )	62.59	60.62	58.18	56.93	60.28	58.76	62.19	58.09	56.48	56.83	590.95	59.10
w(Al <sub>2</sub> O <sub>3</sub> )	16.24	16.29	16.83	16.72	15.90	16.17	15.73	17.88	17.04	16.85	165.65	16.57
w(TFeO)	5.25	5.23	5.74	7.14	5.62	6.15	5.00	4.51	6.54	5.84	57.02	5.70
w(CaO)	4.22	4.73	6.93	6.51	5.58	5.75	4.92	4.70	6.55	7.39	57.28	5.73
w(MgO)	1.92	2.50	2.40	2.77	2.26	2.53	1.83	2.42	2.61	2.43	23.67	2.37
w(Na <sub>2</sub> O)	3.90	3.82	4.02	3.84	3.96	4.21	3.77	3.12	3.99	3.89	38.52	3.85
w(K <sub>2</sub> O)	2.77	3.27	2.57	2.82	2.91	3.05	3.37	2.97	2.56	2.97	29.26	2.93
w(Cr <sub>2</sub> O <sub>3</sub> )	0.01	0.01	0.01	0.01	0.01	0.01	0.01	0.01	0.01	0.01	0.10	0.01
w(TiO <sub>2</sub> )	0.66	0.80	0.82	0.88	0.77	0.85	0.67	0.80	0.96	0.90	8.11	0.81
w(MnO)	0.05	0.06	0.07	0.09	0.10	0.06	0.08	0.01	0.07	0.07	0.66	0.07
w(P <sub>2</sub> O <sub>5</sub> )	0.30	0.34	0.38	0.38	0.32	0.35	0.26	0.34	0.41	0.40	3.48	0.35
w(SrO)	0.10	0.09	0.11	0.11	0.08	0.10	0.08	0.07	0.11	0.10	0.95	0.10
w(BaO)	0.09	0.10	0.08	0.10	0.08	0.08	0.07	0.04	0.07	0.07	0.78	0.08
w(LOI)	1.15	1.44	0.97	0.80	1.39	1.67	0.54	3.81	1.76	1.04	14.57	1.46
Total	99.22	99.29	99.12	99.10	99.26	99.74	98.50	98.74	99.14	98.77	990.88	99.09
w(Na <sub>2</sub> O)+ w(K <sub>2</sub> O)	6.67	7.09	6.59	6.66	6.87	7.26	7.14	6.09	6.55	6.86	67.78	6.78
w(K <sub>2</sub> O)/ [w(Na <sub>2</sub> O)+ w(K <sub>2</sub> O)]	0.42	0.46	0.39	0.42	0.42	0.42	0.47	0.49	0.39	0.43	4.32	0.43
w(Na <sub>2</sub> O)/ w(K <sub>2</sub> O)	1.41	1.17	1.56	1.36	1.36	1.38	1.12	1.05	1.56	1.31	13.28	1.33
A/CKN	0.95	0.88	0.77	0.79	0.80	0.78	0.84	1.06	0.80	0.73	8.40	0.84
A/NK	1.73	1.66	1.79	1.79	1.65	1.58	1.60	2.14	1.83	1.75	17.51	1.75
$\sigma$	2.27	2.85	2.86	3.18	2.73	3.34	2.66	2.46	3.18	3.40	28.94	2.89
$\tau$	18.70	15.59	15.62	14.64	15.51	14.07	17.85	18.45	13.59	14.40	158.41	15.84
AR	1.97	2.02	1.77	1.80	1.94	1.99	2.06	1.74	1.77	1.79	18.84	1.88
Calcium rate	0.37	0.38	0.46	0.39	0.41	0.40	0.42	0.40	0.42	0.47	0.41	0.41

Tested by Guangzhou Aoshi Mineral Laboratory(2011); Analysis method: X-fluorescence spectrum analysis; A/NK= $n(\text{Al}_2\text{O}_3)/[n(\text{Na}_2\text{O})+n(\text{K}_2\text{O})]$ , A/CKN= $n(\text{Al}_2\text{O}_3)/[n(\text{CaO})+n(\text{Na}_2\text{O})+n(\text{K}_2\text{O})]$  (mole ratio of oxide molecular);  $\sigma=[w(\text{Na}_2\text{O})+w(\text{K}_2\text{O})]^2/[w(\text{SiO}_2)-43]$ ;  $\tau$  is Cottine index; AR= $[w(\text{Al}_2\text{O}_3)+w(\text{CaO})+w(\text{Na}_2\text{O})+w(\text{K}_2\text{O})]/[w(\text{Al}_2\text{O}_3)+w(\text{CaO})-(w(\text{Na}_2\text{O})+w(\text{K}_2\text{O}))]$

(w(Na<sub>2</sub>O)+w(K<sub>2</sub>O)) is 6.09%–7.26%, averaging 6.78%. w(Na<sub>2</sub>O)/w(K<sub>2</sub>O) value is 1.05–1.56, averaging 1.33. The content of K<sub>2</sub>O is in the range of 2.56% to 3.27%, averaging 2.93%, higher than the K<sub>2</sub>O content of Chinese diorite (2.65%). The intrusion bears high-K features in a Na-rich background. The alkalic rate (AR) is in the range of 1.74 to 2.06, averaging 1.88. The enrich calcium rate (w(CaO)/[w(CaO)+w(MgO)+w(FeO)+w(MnO)+w(Fe<sub>2</sub>O<sub>3</sub>)] is in the range of 0.37 to 0.47, averaging 0.41, which is slightly higher than the average value of Chinese diorite (0.34) and the average value of Chinese quartz diorite (0.34). The Rittmann combination index ( $\sigma$ ) is in the range of 2.27 to 3.40, averaging 2.89, belonging to calc-alkaline rock. In the w(K<sub>2</sub>O)–w(SiO<sub>2</sub>) diagram (Fig. 4), the rock samples all fall into the high-K

calc-alkaline series, indicating that the rocks of this area are high-K calc-alkaline rocks. Aluminum saturation index (ACNK) averages 0.84, which is lower than 1.1. In the A/NK–A/CNK diagram (Fig. 5), most samples are projected in the quasi-aluminous range, belonging to quasi-aluminous rock. The rocks of this area have high Na/K mole ratio value (averaging 1.33). In the w(Na<sub>2</sub>O)–w(K<sub>2</sub>O) diagram (Fig. 6), the rock samples are all projected in I-type granite zone, showing that the rocks of the area belong to typical I-type granite, indicating the plutonic source of rock-forming materials.

From the Harker diagram (Fig. 7), it is indicated that as the content of SiO<sub>2</sub> increases, the contents of Al<sub>2</sub>O<sub>3</sub>, TFeO, MgO, CaO, TiO<sub>2</sub> and P<sub>2</sub>O<sub>5</sub> decrease,

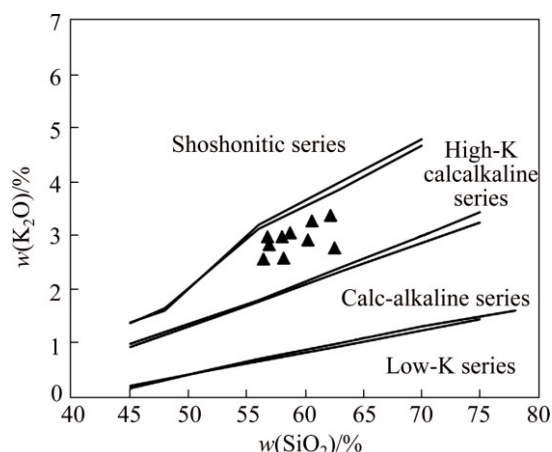


Fig. 4  $w(\text{K}_2\text{O})$ – $w(\text{SiO}_2)$  diagram of Qingshanjiao intrusion (after ROLLINSON [16])

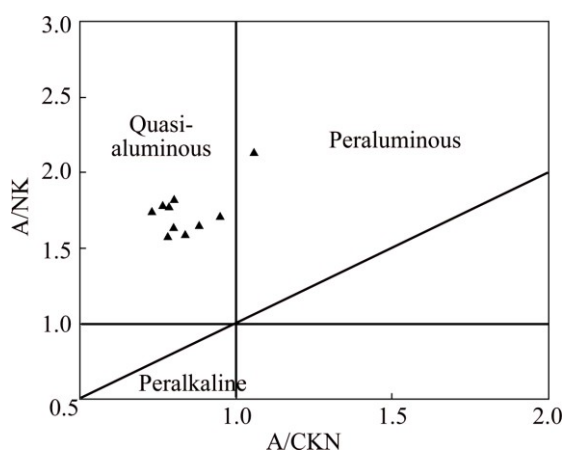


Fig. 5  $A/NK$ – $A/CKN$  diagram of Qingshanjiao rockbody (after MANIAR and PICCOLI [17])

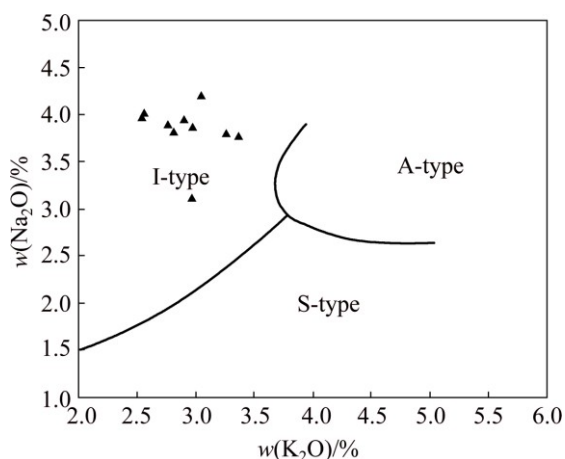


Fig. 6  $w(\text{Na}_2\text{O})$ – $w(\text{K}_2\text{O})$  diagram of Qingshanjiao intrusion (after COLLINS et al [18])

having negative correlation with  $\text{SiO}_2$ , and the content of  $\text{K}_2\text{O}$  increases, having positive correlation with  $\text{SiO}_2$ , indicating that the Qingshanjiao intrusion is the product of evolution of homologous magma and contemporary magma.

### 3.3 Geochemical features of rare earth elements

Existing test results (Table 2) show that the mass fraction range of total rare earth element ( $\sum w(\text{REE})$ ) is from  $192.19 \times 10^{-6}$  to  $314.82 \times 10^{-6}$ , averaging  $230.42 \times 10^{-6}$ , which is lower than that of the world granitic rocks. The range of light rare earth ( $w(\text{LREE})$ ) is from  $158.92 \times 10^{-6}$  to  $275.31 \times 10^{-6}$ , averaging  $192.97 \times 10^{-6}$ . The range of heavy rare earth ( $w(\text{HREE})$ ) is from  $31.80 \times 10^{-6}$  to  $40.13 \times 10^{-6}$ , averaging  $37.45 \times 10^{-6}$ . The range of ratio of light rare earth to heavy rare earth ( $w(\text{LREE})/w(\text{HREE})$ ) is from 4.54 to 6.97, averaging 5.15, which is much higher than 1, showing that light rare earth is relatively strongly enriched.

The range of  $w(\text{Ce})_N/w(\text{Yb})_N$  value is from 7.68 to 12.28, averaging 9.21, which is much higher than 1, indicating that the rocks are rich in rare earth. The range of  $w(\text{Gd})_N/w(\text{Yb})_N$  value is from 1.40 to 1.70, averaging 1.58, which is smaller than average  $w(\text{La})_N/w(\text{Sm})_N$  (4.50), indicating that fractionation degree of heavy rare earth elements is low, and is slower in decay compared with light rare earth elements. The range of Eu anomaly value ( $\delta(\text{Eu})$ ) is from 0.75 to 1.18, averaging 1.01, showing that overall Eu anomaly is not obvious, indicating that the rock belongs to non-Eu-anomaly type (normal type); the range of Ce anomaly value ( $\delta(\text{Ce})$ ) is from 0.81 to 0.88, averaging 0.84, which is small in variation, showing that Ce anomaly is not obvious. These indicate that the rock belongs to Ce weakly deficit type, and that the rock is weakly influenced by surface weathering. The distribution curves of porphyritic granodiorite and quartz monzonite almost overlap each other, showing that the rocks of different output phases have the same material source.

Qingshanjiao intrusion has higher  $w(\text{La})_N/w(\text{Yb})_N$  ratio, but depleted in heavy rare earth element abundances. It is confirmed that the magma is not likely to derive from partial melting of the lower crust which consists of granulite facies rocks, and is not the source of the upper crust.

### 3.4 Geochemical features of trace elements

In order to ensure concordant standard with REE and avoid human factor in the primitive mantle model, chondrite value provided by THOMPSON [19] was adopted for normalization. Trace element spider diagram (Fig. 8) is made based on the analysis results (Table 3). It shows that the rocks in this area are enriched in large-ion lithophile elements such as Rb, Sr and Th, but depleted in high field strength elements such as Nb, Ti and Ta. Enrichment of large-ion lithophile elements demonstrates that the rock-forming materials derive from low-grade melting of upper mantle. Deficit of high field strength elements demonstrates the existence of contamination from crust materials [20]. The Nb, Ti and Y contents

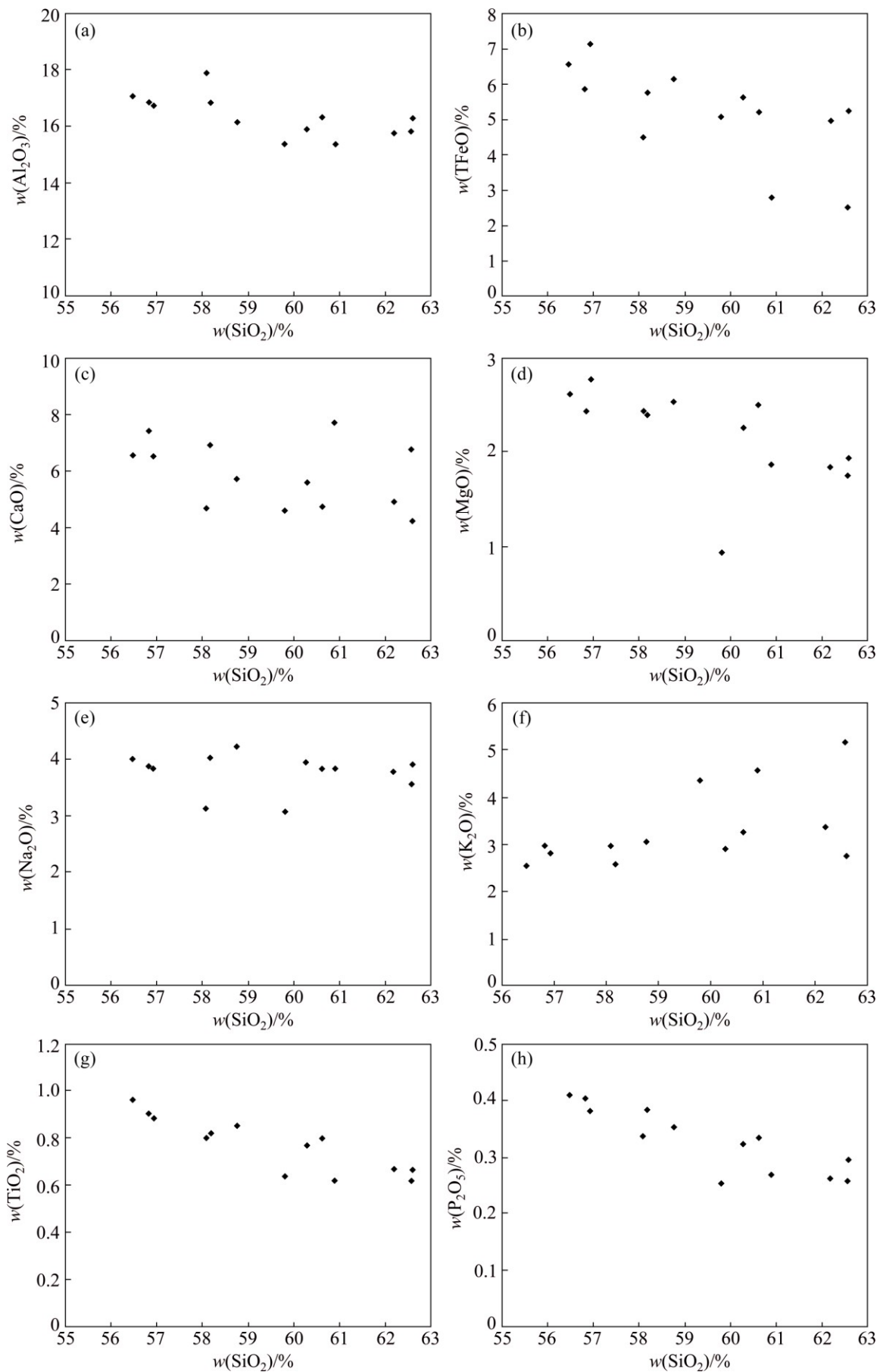


Fig. 7 Harker diagram of Qingshanjiao intrusion

**Table 2** Content table of rare earth elements of Qingshanjiao intrusion (mass fraction,  $10^{-6}$ )

Parameter	TS003-1	DK001-4	DK004-3	DK004-4	DK004-5	DK005-1	DGS8-11	DGS3-11	DGS8-8	ZK-51	Average value
w(La)	46.90	40.10	43.80	38.60	40.60	42.30	44.30	72.70	48.00	52.70	47.00
w(Ce)	92.40	79.00	93.30	74.00	76.90	84.00	82.60	130.00	94.10	101.50	90.78
w(Pr)	9.94	8.75	10.75	8.07	8.24	9.18	9.05	13.70	10.60	11.25	9.95
w(Nd)	35.80	31.90	41.60	30.90	30.30	34.10	32.20	49.30	40.60	42.20	36.89
w(Sm)	6.70	5.84	7.73	5.51	5.15	6.38	5.51	8.02	7.27	7.35	6.55
w(Eu)	1.68	1.63	2.04	1.84	1.58	1.80	1.63	1.59	2.09	2.14	1.80
w(Gd)	5.56	4.69	6.09	4.74	4.31	5.05	4.55	5.49	5.36	5.35	5.12
w(Tb)	0.77	0.64	0.82	0.64	0.57	0.77	0.65	0.74	0.73	0.72	0.71
w(Dy)	4.21	3.73	4.95	3.62	3.61	4.17	3.60	4.37	4.32	4.27	4.09
w(Ho)	0.85	0.72	0.86	0.73	0.73	0.77	0.72	0.81	0.80	0.78	0.78
w(Er)	2.14	1.99	2.63	1.94	1.71	2.38	1.94	2.29	2.32	2.27	2.16
w(Tm)	0.34	0.26	0.40	0.31	0.31	0.35	0.28	0.35	0.33	0.34	0.33
w(Yb)	2.10	1.71	2.37	1.71	1.69	2.21	1.91	2.14	2.06	2.04	1.99
w(Lu)	0.34	0.26	0.34	0.28	0.27	0.33	0.30	0.32	0.31	0.32	0.31
w(Y)	23.50	19.80	25.40	19.30	18.60	22.60	20.30	23.00	23.90	23.30	21.97
$\sum w(\text{REE})$	233.23	201.02	243.08	192.19	194.57	216.39	209.54	314.82	242.79	256.53	230.42
w(LREE)	193.42	167.22	199.22	158.92	162.77	177.76	175.29	275.31	202.66	217.14	192.97
w(HREE)	39.81	33.80	43.86	33.27	31.80	38.63	34.25	39.51	40.13	39.39	37.45
w(LREE)/w(HREE)	4.86	4.95	4.54	4.78	5.12	4.60	5.12	6.97	5.05	5.51	5.15
$\delta(\text{Eu})$	0.89	1.01	0.96	1.18	1.09	1.02	1.06	0.75	1.07	1.09	1.01
$\delta(\text{Ce})$	0.86	0.85	0.88	0.84	0.84	0.86	0.82	0.81	0.84	0.84	0.84
$w(\text{La})_{\text{N}}/w(\text{Yb})_{\text{N}}$	13.26	13.92	10.97	13.40	14.26	11.36	13.77	20.17	13.83	15.34	14.03
$w(\text{Ce})_{\text{N}}/w(\text{Yb})_{\text{N}}$	8.89	9.34	7.96	8.75	9.20	7.68	8.74	12.28	9.23	10.06	9.21
$w(\text{La})_{\text{N}}/w(\text{Sm})_{\text{N}}$	4.38	4.29	3.54	4.38	4.93	4.14	5.02	5.67	4.13	4.48	4.50
$w(\text{Gd})_{\text{N}}/w(\text{Yb})_{\text{N}}$	1.62	1.68	1.57	1.70	1.56	1.40	1.46	1.57	1.59	1.61	1.58

**Table 3** Content table of trace element of Qingshanjiao intrusion (mass fraction,  $10^{-6}$ )

Parameter	TS003-1	DK001-4	DK004-3	DK004-4	DK004-5	DK005-1	DGS8-11	DGS3-11	DGS8-8	ZK-51
w(Rb)	118.00	142.00	82.60	83.50	92.60	94.40	108.50	192.50	64.70	73.70
w(Ba)	861.00	939.00	783.00	951.00	704.00	748.00	823.00	536.00	748.00	832.00
w(Th)	9.26	7.63	7.45	5.68	8.78	10.25	14.60	11.65	9.50	8.97
w(Ta)	1.00	1.00	1.20	0.60	0.90	1.00	1.10	1.10	1.00	1.00
w(K)	22700.00	26500.00	21200.00	23400.00	23900.00	24600.00	29700.00	25000.00	21400.00	30100.00
w(Nb)	14.50	14.40	17.60	11.10	13.10	13.40	15.90	16.30	15.10	15.30
w(La)	46.90	40.10	43.80	38.60	40.60	42.30	30.00	40.00	40.00	40.00
w(Ce)	92.40	79.00	93.30	74.00	76.90	84.00	82.60	130.00	94.10	101.50
w(Sr)	899.00	801.00	942.00	969.00	710.00	857.00	715.00	650.00	1005.00	1020.00
w(Nd)	35.80	31.90	41.60	30.90	30.30	34.10	32.20	49.30	40.60	42.20
w(P)	1310.00	1460.00	1690.00	1680.00	1420.00	1510.00	1230.00	1630.00	1960.00	1960.00
w(Zr)	192.00	199.00	243.00	231.00	182.00	172.00	197.00	233.00	243.00	241.00
w(Hf)	5.40	5.30	6.50	6.00	5.20	4.90	5.70	6.00	6.10	6.00
w(Sm)	6.70	5.84	7.73	5.51	5.15	6.38	5.51	8.02	7.27	7.35
w(Ti)	3800.00	4200.00	4600.00	5100.00	4400.00	4700.00	3900.00	3900.00	5500.00	5500.00
w(Tb)	0.77	0.64	0.82	0.64	0.57	0.77	0.65	0.74	0.73	0.72
w(Y)	23.50	19.80	25.40	19.30	18.60	22.60	20.30	23.00	23.90	23.30
w(Yb)	2.10	1.71	2.37	1.71	1.69	2.21	1.91	2.14	2.06	2.04
$w(\text{Rb})_{\text{N}}/w(\text{Yb})_{\text{N}}$	35.32	52.20	21.91	30.69	34.44	26.85	35.71	56.54	19.74	22.71
K*	1.96	2.57	1.83	2.65	2.37	2.30	3.39	2.36	2.08	2.92
Nb*	0.25	0.24	0.32	0.20	0.23	0.23	0.27	0.28	0.29	0.23
Zr*	1.30	1.32	1.35	1.38	1.27	1.06	1.47	1.37	1.25	1.25
Ti*	0.26	0.33	0.28	0.42	0.39	0.33	0.32	0.23	0.36	0.35

K\*= $2K_{\text{N}}/(Ta_{\text{N}}+La_{\text{N}})$ ; Nb\*= $2Nb_{\text{N}}/(K_{\text{N}}+La_{\text{N}})$ ; Zr\*= $2Zr_{\text{N}}/(P_{\text{N}}+Sm_{\text{N}})$ ; Ti\*= $2Ti_{\text{N}}/(Sm_{\text{N}}+Tb_{\text{N}})$

of the rocks are lower compared with Vickers value, while Sr content is higher, which is prominently different from continental crust derived granite. Enrichment of Rb and deficit of Nb and Ta demonstrate that the magma is subjected to contamination from crust material during ascending, which are compliant with the conclusions from petrochemical characteristics.

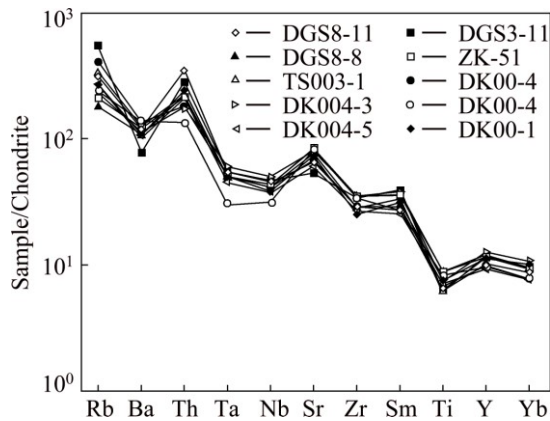


Fig. 8 Trace element spider diagram of Qingshanjiao intrusion

Anomaly values of trace elements,  $w(\text{Rb})_N/w(\text{Yb})_N$ ,  $K^*$ ,  $Zr^*$ ,  $Nb^*$  and  $Ti^*$  are usually used in the study of the rock-forming material source and diagenesis environment [20]. The  $w(\text{Rb})_N/w(\text{Yb})_N$  values of rocks in Qingshanjiao intrusion range from 19.74 to 52.20 (Table 3), indicating that the rock-forming material is mainly derived from low-grade melting of enriched mantle. The  $K^*$ ,  $Zr^*$ ,  $Nb^*$  and  $Ti^*$  are 1.83–2.92, 1.06–1.47, 0.20–0.32 and 0.23–0.42, respectively, indicating the crust source characteristics. These show that the rock-forming material is derived from crust–mantle mixed source.

## 4 Discussion on rock-forming mechanism

### 4.1 Derivation of magma

There are different opinions for the magma source of Tongling ore district: 1) the magma is the product of melting of old lower mantle [21–28], and XU [24] suggested that the mantle involved in the formation of magma in the form of energy; 2) the magma is the product of upper mantle alkaline basaltic magma assimilated older crust material [1,29–34]; 3) the magma is the product of crust–mantle interaction [3,8,9,35–40]. WU et al [4] suggested that the kohalaite series rocks might be the products of differentiation of mantle-derived alkaline basaltic magma, and the high-K calc-alkaline series rocks might be the products of the mantle magma and crust magma mixing; 4) the magma is the product of evolution of adakitic magma derived from partial melting of subducting oceanic crust [41–43].

XU et al [39] excluded the possibility that the

magma of Tongling area is derived from crust melting from Sr, Nd isotope composition. The fact that intrusion does not have negative Eu anomaly indicates that there is no large-scale fractional crystallization of plagioclase. XIE et al [40] indicate that there is small possibility that the medium-acidic intrusive rocks are formed from fractional crystallization of basic magma. Qingshanjiao intrusion is characterized by high-K, alkali-rich,  $A/\text{CNK} < 1.1$  and high Na/K mass ratio, belonging to high-K calc-alkaline series, and is typical I-type granite, which suggests that the magma source is mainly from mantle and lower crust [44]. The trace elements suggest that the Qingshanjiao intrusion is enriched in large-ion lithophile elements Rb, Sr and Th, and depleted in high field-strength elements Nb, Ti and Ta. The abundances of Sr element are consistent with the mantle-derived alkaline basalt. The average value of  $(\sum w(\text{REE}))$  is  $230.42 \times 10^{-6}$ , which is relatively low. Light rare earth is relatively enriched, with high  $w(\text{La})_N/w(\text{Yb})_N$  ratio, indicating that the mantle-derived magma is joined by crust-derived materials, which is supported by the trace element anomaly value of  $w(\text{Rb})_N/w(\text{Yb})_N > 1$ ,  $K^* > 1$ ,  $Zr^* > 1$ ,  $Nb^* < 1$  and  $Ti^* < 1$  [21]. The above characteristics indicate that the primary magma has the feature of mantle–crust mixing, and is the product of mixing of mantle-derived material and crust-derived material. Besides, the zircon of this area has lots of new Proterozoic ((747–823) Ma) and Archean zircon core ( $2196 \pm 15$ ) Ma [4,44]. However, the contamination of lower crust could only cause the intrusion to inherit a small amount of old zircon core. Therefore, it is indicated that lots of lower-crust materials participate in the magmatism [4,45]. The existence of magma mixing structure in the intrusion showed that the Yanshanian magmatism in this area experienced mixing process of mantle-derived material and crust-derived material [36,39,40,46]. The existence of potash feldspar poikilitic texture in the fine ultramafic inclusions showed that the basaltic magma experienced a mixing process with a type of alkali-rich magma (primarily inferred as syenite magma) [45]. Therefore, it is considered that the primary magma is likely a product of mixing between basaltic magma and syenite magma formed from melting of lower crust.

### 4.2 Petrogenic and geodynamic setting

The Cottine index ( $\tau$ ) is an important parameter used to reflect the volcano rock formation environment.  $\tau < 10$  represents stable non-orogenic belt environment, whereas  $\tau > 10$  represents strong active continental margin (orogenic belt) environment [47]. The Cottine index of the rocks in this area averages 15.84, which is higher than 10, indicating a non-stable environment. Based on  $\lg \tau - \lg \sigma$  relationship diagram, the tectonic units of

ingeneous formation can be divided. In the  $\lg \tau$ – $\lg \sigma$  relationship diagram (Fig. 9), all the samples fall into volcanic rock of orogenic belt zone (Zone B). In the  $w(\text{Nb})$ – $w(\text{Y})$  relationship diagram (Fig. 10), the samples are located in the collision granite and oceanic-ridge granite zone, indicating that the formation of intrusion is closely related to orogenic belt or plate collision, which is also supported by the depleted Nb and Ta of Qingshanjiao intrusion. It is enriched in Rb, and depleted in Ti, which is similar to post collision granite. This shows that the rock-forming environment is transition environment from compressional to extensional [50,51].

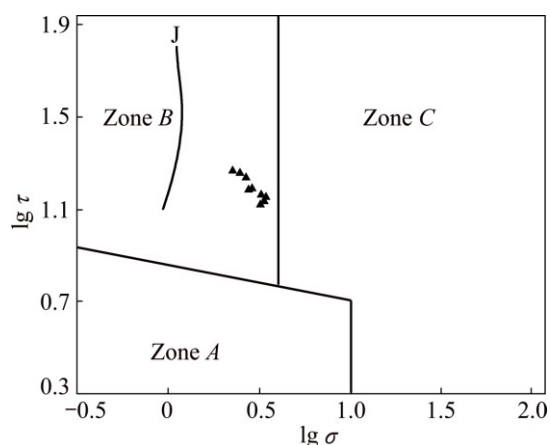


**Fig. 9**  $\lg \tau$ – $\lg \sigma$  relationship diagram of Qingshanjiao intrusion (after RITTMANN [48]): Zone A–Igneous rock from non-orogenic zones; Zone B–Igneous rock from orogenic belt (island-arc and active continental edge); Zone C–Alkaline rock derived from Zones A and B

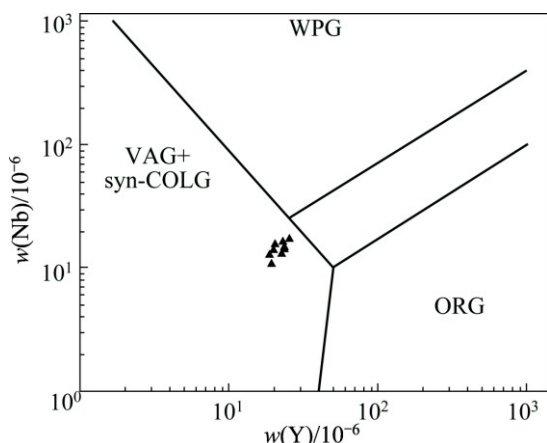


**Fig. 10**  $w(\text{Nb})$ – $w(\text{Y})$  relationship diagram of Qingshanjiao intrusion (after Pearce [49]): VAG–Volcanic-arc granite; COLG–Collision granite; WPG–Within-plate granite; ORG–Oceanic-ridge granite

### 4.3 Rock-forming process

From Harker diagram (Fig. 7), it can be seen that as the content of  $\text{SiO}_2$  increases, the  $\text{TFeO}$ ,  $\text{MgO}$ ,  $\text{CaO}$ ,  $\text{TiO}_2$  and  $\text{P}_2\text{O}_5$  contents decrease, showing negative

correlation with  $\text{SiO}_2$  content, indicating that the fractional crystallization of mafic minerals (pyroxene, hornblende, ilmenite and apatite) plays an important role during the magmatic evolution process [7,14,39]. The  $w(\text{CaO})/w(\text{Na}_2\text{O})$  ratio is positively correlated with the  $\text{CaO}$  content (Fig. 11), which also indicates that fractional crystallization of clinopyroxene occurs during the magmatic evolution process [6]. Hybrid textures including plagioclase zoning, plagioclase intercalary crystal and feldspar potash intercalary crystal are observed in Qingshanjiao intrusion (Figs. 3(a) and (b)), indicating that fractional crystallization during the magmatic evolution process has caused regular variation and distribution of major elements and trace elements [40]. The  $\text{K}_2\text{O}$  content increases and is positively correlated with  $\text{SiO}_2$  content.  $\text{Na}_2\text{O}$  is not clearly related with  $\text{SiO}_2$  content. These indicated that fractional crystallization of K-depleted minerals occurred during the magmatic evolution process, or that potassic alteration occurred to the intrusion.

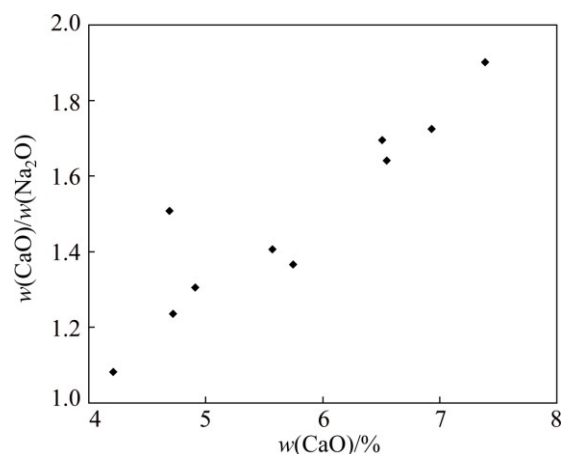


**Fig. 11**  $w(\text{CaO})/w(\text{Na}_2\text{O})$ – $w(\text{CaO})$  relationship diagram of Qingshanjiao intrusion

The sample points in the  $w(\text{La})_{\text{N}}/w(\text{Sm})_{\text{N}}$ – $w(\text{La})$  relationship diagram (Fig. 12) are arranged in an oblique line during the partial melting process, and a horizontal line during fractional crystallization process. From Fig. 12, it can be seen that the sample projection point in this area is neither an oblique line nor a horizontal line. The linear relationship is not obvious. Therefore, the magmatic evolution process is not simply partial melting or fractional crystallization, instead, it is a relatively complicated rock-forming process, and there might be participation of crust material during the magmatic evolution process.

Beside  $\text{Al}_2\text{O}_3$  and  $\text{MgO}$ , the rock consolidation index  $\lg S_1$  is not clearly related to the contents of  $\text{SiO}_2$ ,  $\text{Fe}_2\text{O}_3$ ,  $\text{CaO}$ ,  $\text{Na}_2\text{O}$  and  $\text{K}_2\text{O}$ , demonstrating that assimilation and contamination might occur between Qingshanjiao intrusion and wall rock during the

magmatic evolution process, as suggested by ZHOU et al [52].

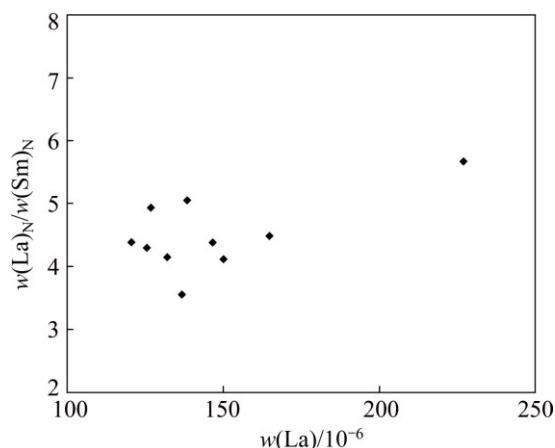


Fig. 12  $w(\text{La})_N/w(\text{Sm})_N-w(\text{La})$  relationship diagram of Qingshanjiao intrusion

#### 4.4 Discussion on rock-forming mechanism

Under the dynamic background of continental collision and extension between the Yangtze plate and northern China plate since Triassic period [53], the crust–mantle mixed primitive magma increased to the deep crust and formed deep magma chamber. The primary magma formed the intermediary-basic magma by fractional crystallization and assimilation and hybridization with sima layer material of lower crust. With further increase of the intermediary-basic magma, the temperature decreased, the magma started to separate ferromagnesian, assimilation and hybridization with mid-shallow crust material occurred, and the intermediate-acidic magma formed. During the intermediary-acidic magma ascended and intruded, deep dikes were formed in upper crust. Under the effect of tectonic movement and high pressure, the magma continued to increase and apophyses formed on shallow surface. Due to the inflow of external fluid and change of its own physical and chemical conditions, potassium alteration, propylitization, argillization and metal sulfides mineralization occurred inside the intrusion. Skarnization and retrograde alteration of early skarn occurred in the contact zone between the intrusion and the wall rock and its adjacent area.

Petrochemistry of Qingshanjiao intrusion shows that as the  $\text{SiO}_2$  content increases,  $\text{Al}_2\text{O}_3$ ,  $\text{TFeO}$ ,  $\text{MgO}$ ,  $\text{CaO}$ ,  $\text{TiO}_2$  and  $\text{P}_2\text{O}_5$  contents decrease.  $\text{K}_2\text{O}$  content increases, showing positive correlation with  $\text{SiO}_2$  content. These showed that besides fractional crystallization within the magma, assimilation and hybridization with crust-derived material also occurred during the magma evolution process. The range of calcium enrichment rate  $w(\text{CaO})/[w(\text{CaO})+w(\text{MgO})+w(\text{FeO})+w(\text{MnO})+w(\text{Fe}_2\text{O}_3)]$  of Qingshanjiao intrusion is from 0.37 to 0.47, averaging

0.41, which is a bit higher than the average value of China diorite (0.34) and China quartz diorite (0.34). This indicated that certain degree of assimilation and hybridization occurred between the magma and the calcareous wall rock strata during the magma evolution process. Therefore, the intrusion in this area was formed by mixing the mantle-derived magma with crustal rocks under the extensional environment after the collision, based on its own fractional crystallization and assimilation and hybridization with crust-derived material.

Trace elements and H–O, S and Pb isotope test results [10,54] show that the mineralization in this area has a close genetic relation with Yanshanian magmatism. The magmatism offers many metallogenic materials, ore-forming fluids and heat energy. The Qingshanjiao intrusion of Yanshanian is the primary factor for mineralization. Near the Qingshanjiao intrusion, the thickness of ore body increased, ore grade turned to be higher. And the Qingshanjiao is the host intrusion for porphyry type copper–gold ore body.

## 5 Conclusions

1) The Qingshanjiao intrusion enriched in large-ion lithophile elements, depleted in high field strength elements. The trace element anomaly values  $w(\text{Rb})_N/w(\text{Yb})_N > 1$ ,  $\text{K}^* > 1$ ,  $\text{Zr}^* > 1$ , and  $\text{Nb}^* < 1$ ,  $\text{Ti}^* < 1$ . The light rare earth elements are enriched and heavy rare earth elements are depleted. The  $w(\text{La})_N/w(\text{Yb})_N$  ratio is higher, indicating high degree of differentiation. These indicate the source rock with mantle–crust mixed characteristics.

2) The primary magma of forming the Qingshanjiao intrusion is a mixed product between mantle-derived basaltic magma and syenite magma from partial melting of lower crust materials. The rock-forming environment is conversion environment from compression to extension during the period from late Jurassic to early Cretaceous.

3) The relationship between the oxides and trace elements of the intrusion demonstrated that both fractional crystallization and assimilation and contamination occurred during the magma evolution process. Plagioclase zoning, plagioclase intercalary crystal and feldspar potash intercalary crystal show that the fractional crystallization during the magma evolution caused regular change and distribution of major elements and trace elements.

4) The mantle–crust mixed magma differentiated and evolved under the conversion environment from compression to extension. Fractional crystallization and assimilation and contamination occurred during this process. The Qingshanjiao intrusion was formed under

the combined control of the fractional crystallization and assimilation and contamination.

## References

- [1] TANG Yong-cheng, WU Yan-chang, CHU Guo-zheng, XING Feng-ming, WANG Yong-min, CAO Fen-yang, CHANG Yin-fo. Geology of copper-polymetallic deposits along the Yangtze River of Anhui province [M]. Beijing: Geological Publishing House, 1998: 1–351. (in Chinese)
- [2] WU Cai-lai, DONG Shu-wen, GUO He-ping, GUO Xiang-yan, GAO Qian-ming, LIU Liang-gen, CHEN Qi-long, LEI Min, WOODEN J L, MAZADAB F K, MATTINSON C. Zircon SHRIMP U–Pb dating of intrusive rocks and hypomagmatic process from Shizishan, Tongling [J]. Acta Petrol Sinica, 2008, 24(8): 1801–1812. (in Chinese)
- [3] WU Cai-lai, GAO Qian-ming, GUO He-ping, GUO Xiang-yan, LIU Liang-gen, HAO Yuan-hong, LEI Min, QIN Hai-peng. Petrogenesis of the intermediate-acid intrusive rocks and zircon SHRIMP dating in Tongling, Anhui, China [J]. Acta Petrol Sinica, 2010, 26(8): 2630–2652. (in Chinese)
- [4] WU Cai-lai, ZHOU Ruo, HUANG Xu-chen, ZHANG Cheng-huo, HUANG Wen-ming. Zircon U–Pb dating of high-K calc-alkaline intrusive rocks from Tongling: Implications for the tectonic setting [J]. Geochimica, 2013, 42(1): 11–28. (in Chinese)
- [5] HUANG Shun-sheng, XU Zhao-wen, GU Lian-xing, HUA Ming, LU Xian-cai, LU Jian-jun, NIE Gui-ping, ZHU Shi-peng. A discussion on geochemical characteristics and genesis of intrusions in Shizishan orefield, Tongling area, Anhui province [J]. Geological Journal of China Universities, 2004, 10(2): 217–226. (in Chinese)
- [6] XIE Jian-cheng, YANG Xiao-yong, DU Jian-guo, SUN Wei-dong. Zircon U–Pb geochronology of the Mesozoic intrusive rocks in the Tongling region: Implications for copper-gold mineralization [J]. Acta Petrol Sinica, 2008, 24(8): 1782–1800. (in Chinese)
- [7] XU Xiao-chun, LIU Qi-neng, ZHANG Zhan-zhan, WANG Ping, XIAO Qiu-xiang, LIANG Jian-feng. Anhui Tongling ore deposits: The series and formation of dioritic intrusive rock related to mineralization in Tongling ore cluster region, Anhui province [J]. Acta Mineralogica Sinica, 2011, 31(S1): 112–113. (in Chinese)
- [8] GUO Wei-min, LU Jian-jun, JIANG Shao-yong, ZHANG Rong-qing, ZHAO Zhan-jie. Chronology, Hf isotopes, geochemistry, and petrogenesis of the magmatic rocks in the Shizishan ore field of Tongling, Anhui province [J]. Science China (Earth Sciences), 2013, 43(8): 1268–1286. (in Chinese)
- [9] WANG Shi-wei, ZHOU Tao-fa, YUAN Feng, FAN Yu, ZHANG Le-jun, SONG Yu-long. Petrogenesis of Dongguashan skarn-porphphyry Cu–Au deposit related intrusion in the Tongling district, eastern China: Geochronological, mineralogical, geochemical and Hf isotopic evidence [J]. Ore Geology Review, 2015, 64, 53–70.
- [10] LIU Zhong-fa, SHAO Yong-jun, ZHOU Xin, ZHANG Yu, ZHOU Gui-bin. Hydrogen, oxygen, sulfur and lead isotope composition tracing for the ore-forming material source of Dongguashan copper (gold) deposit in Tongling, Anhui Province [J]. Acta Petrologica Sinica, 2014, 30(1): 199–208. (in Chinese)
- [11] WU Cai-lai, ZHOU Ruo, HUANG Xu-chen, ZHANG Cheng-huo, HUANG Wen-ming.  $^{40}\text{Ar}/^{39}\text{Ar}$  chronology of intermediate-acid intrusive rocks from Tongling [J]. Acta Petrol Mineral, 1996, 15(4): 299–306. (in Chinese)
- [12] XU Zhao-wen, FANG Chang-quan, LU Xian-cai, LU Jian-jun, JIANG Shao-yong, GAO Geng, WANG Yun-jian. Study on genetic mechanism of magmatic rocks of Shizishan ore field in Tongling [C]//Proceedings of the Third Symposium Igneous Rocks Granite Genesis and Crustal Evolution. Nanjing: Nanjing University Press, 2004: 117–119.
- [13] LU San-ming. The magmatism and fluid mineralization Shizishan copper–gold ore-field of Tongling, Anhui, province [D]. Hefei: Hefei University of Technology, 2007: 1–158. (in Chinese)
- [14] XU Xiao-chun, LU San-ming, XIE Qiao-qin, LOU Jin-wei, ZHU Ping-li. Trace element geochemical characteristics of fluid inclusions of Dongguashan ore deposit in Tongling, Anhui province, and their geological implications [J]. Acta Petrologica Sinica, 2008, 24(8): 1865–1874. (in Chinese)
- [15] LI Tong. Chemical element abundances in the earth and its majorshells [J]. Geochimica, 1976(3): 167–174. (in Chinese)
- [16] ROLLINSON H R. Using geochemical data: evaluation, presentation, interpretation [M]. New York: Longman Group Ltd., 1993: 352.
- [17] MANIAR P D, PICCOLI P M. Tectonic discrimination of granitoids [J]. Geological Society of America Bulletin, 1989, 101: 635–643.
- [18] COLLINS W J, BEAMS S D, WHITE A J R, CHAPPELL B W. Nature and origin of a type granites with particular reference to Southeastern Australia [J]. Contribution to Mineralogy and Petrology. 1982, 80(2): 189–200.
- [19] THOMPSON R N. Magmatism of the British tertiary volcanic province [J]. Scottish Journal of Geology, 1982, 18(1): 49–107.
- [20] REN Kang-xu, YAN Guo-han, MU Bao-lei, CAI Jian-hui, TONG Ying, LI Feng-tang, ZHAO Feng-san, GU Li-bing, YANG Bin, CHU Zhu-yin. Geochemistry and Nd, Sr, Pb isotopic characteristics of the alkali-rich intrusive rocks in Alxa Fault Block, Western Inner Mongolia and their implications [J]. Earth Science Frontiers, 2005, 12(2): 292–301. (in Chinese)
- [21] WILLSON M. Igneous petrogenesis: A globe tectonic approach [M]. London: Unwin Hyman, 1989: 65–287.
- [22] YANG Xue-ming, LIN Wen-tong. Research on the petrogenic mechanism of the Tongguanshan igneous complex, Anhui Province [J]. Geological Review, 1988, 34(1): 25–35. (in Chinese)
- [23] DU Yang-song, LI Xue-jun. Enclaves in the typical mining districts of Tongling, Anhui and their implication to the process of magmatism-metallogeny [J]. Geological Journal of China Universities, 1997, 3(2): 171–182. (in Chinese)
- [24] XU Qi-dong. Crust–crust mixing source characteristics of Mesozoic granitoids in the middle-lower reaches of the Yangtze River [J]. Acta Petrologica et Mineralogica, 1997, 16(2): 120–130. (in Chinese)
- [25] ZHANG Qi, QIAN Qing, WANG Er-qi, WANG Yan, ZHAO Tai-ping, HAO Jie, GUO Guang-jun. An east China plateau in Mid-Late Yanshanian period: Implication from adakites [J]. Chinese Journal of Geology, 2001, 36(2): 248–255.
- [26] ZHANG Qi, WANG Yan, QIAN Qing, YANG Jin-hui, WANG Yuan-long, ZHAO Tai-ping, GUO Guang-jun. The characteristics and tectonic-metallogenetic significances of the adakites in Yanshan period from eastern China [J]. Acta Petrologica Sinica, 2001, 17(2): 236–244. (in Chinese)
- [27] ZHANG Qi, WANG Yan, WANG Yuan-long. Preliminary study on the components of the lower crust in East China Plateau during Yanshanian: Constraints on Sr and Nd isotopic compositions of adakite-like rocks [J]. Acta Petrologica Sinica, 2001, 17(4): 505–513. (in Chinese)
- [28] WANG Yuan-long, WANG Yan, ZHANG Qi, JIA Xiu-qin, HAN Song. The geochemical characteristics of Mesozoic intermediate-acid intrusives of the Tongling area and its metallogenesis–geodynamic implications [J]. Acta Petrologica Sinica, 2004, 20(2): 325–338. (in Chinese)
- [29] MAO Jian-ren, SU Yu-xiang, CHEN San-yuan. Intermediate acid intrusive and mineralization in the middle-lower reaches of Yangtze River [M]. Beijing: Geological Publishing House, 1990: 1–191. (in Chinese)
- [30] CHEN Jiang-feng, ZHOU Tai-xi, LI Xue-ming, FOLAND K A, HUANG Cheng-yi, LU Wei. Sr and Nd isotopic constraints on source regions of the intermediate and acid intrusions from Southern Anhui Province [J]. Geochimica, 1993, 22(3): 261–268. (in Chinese)
- [31] CHEN J F, JAHN B M. Crustal evolution of Southeastern China: Nd and Sr isotopic evidence [J]. Tectonophysics, 1998, 284(1–2): 101–133.
- [32] XING Feng-ming, XU Xiang. AFC mixing model and origin of intrusive rocks from Tongling area [J]. Acta Petrologica et Mineralogica, 1996, 15(1): 10–20. (in Chinese)

- [33] XING Feng-ming. Geochemistry of basic rocks from the eastern part of the Yangtze magmatic rock belt [J]. *Geochimica*, 1998, 27(3): 258–268. (in Chinese)
- [34] MENG Xiang-jin, LÜ Qing-tian, YANG Zhu-sen, XU Wei-yi. Geochemical characteristics of Mesozoic intermediate-acid intrusive rocks in Tongling and adjacent area of the middle and lower reaches of the Yangtze River and its indication to the deep-seated magmatism [J]. *Acta Geologica Sinica*, 2011, 85(5): 757–777. (in Chinese)
- [35] WANG Qiang, XU Ji-feng, ZHAO Zhen-hua, XIONG Xiao-lin, BAO Zhi-wei. Petrogenesis of the Mesozoic intrusive rocks in the Tongling area, Anhui Province, China and their constraint to geodynamic process [J]. *Science China (D)*, 2003, 33(4): 323–334. (in Chinese)
- [36] DI Yong-jun, ZHAO Hai-ling, WU Gan-guo, ZHANG Da, ZANG Wen-shuang, LIU Qing-hua. Genesis of the intrusive rocks from the Tongling area during the Yanshanian and mixing of three-end-member magma [J]. *Geological Review*, 2005, 51(5): 528–538. (in Chinese)
- [37] DI Yong-jun, ZHAO Hai-ling, ZHANG Yi-quan, ZHAO Jian-hua, YANG Long. Petrographic evidences for magma mixing in the granitoids from Tongling area, Anhui Province [J]. *Beijing Geology*, 2003, 15(1): 12–17. (in Chinese)
- [38] DU Yang-song, QIN Xin-long, CAO Yi. Sulfide and oxide inclusions in xenoliths and host rocks of Tongling area, Anhui Province [J]. *Mineral Deposits*, 2010, 29(1): 71–84. (in Chinese)
- [39] XU Xiao-chun, BAI Ru-yu, XIE Qiao-qin, LOU Jin-wei, ZHANG Zhan-zhan, LIU Qi-neng, CHEN Li-wei. Re-understanding of the geological and geochemical characteristics of the Mesozoic intrusive rocks from Tongling area of Anhui Province, and discussions on their genesis [J]. *Acta Petrologica Sinica*, 2012, 28(10): 3139–3169. (in Chinese)
- [40] XIE Jian-cheng, YANG Xiao-yong, XIAO Yi-lin, DU Jian-guo, SUN Wei-dong. Petrogenesis of the Mesozoic intrusive rocks from the Tongling ore cluster region: The metallogenic significance [J]. *Acta Geologica Sinica*, 2012, 86(3): 423–459. (in Chinese)
- [41] LING M X, WANG F Y, DING X, HU Y H, ZHOU J B, ZARTMAN R E, YANG X Y, SUN W D. Cretaceous ridge subduction along the Lower Yangtze river belt, eastern China [J]. *Economic Geology*, 2009, 104(2): 303–321.
- [42] LING M X, WANG F Y, DING X, ZHOU J B, SUN W D. Different origins of adakites from the Dabie Mountains and the Lower Yangtze River Belt, eastern China: Geochemical constraints [J]. *International Geology Review*, 2011, 53(5–6): 727–740.
- [43] SUN Wei-dong, LING Ming-xing, YANG Xiao-yong, FAN Wei-ming, DING Xing, LIANG Hua-yang. Ridge subduction and porphyry copper gold mineralization [J]. *Science China (Earth Sciences)*, 2010, 40(2): 127–137. (in Chinese)
- [44] CHAPPELL B W, WHITE A J R. Two contrasting granite type [J]. *Pacific Geology*, 1974, 8: 173–175.
- [45] MAO Jing-wen, HU Rui-zhong, CHEN Yu-chuan, WANG Yi-tian. Large-scale metallogenesis and large clusters of mineral deposits [M]. Beijing: Geological Publishing House, 2006: 1–533. (in Chinese)
- [46] WU C L, WANG Z H, QIAO D W, LI H B, HAO M Y, SHI R D. Types of enclaves and their features and origins in intermediate-acid intrusive rocks from Tongling district, Anhui province, China [J]. *Acta Geologica Sinica*, 2000, 74(1): 54–67.
- [47] QU Hong-ying, CHANG Guo-xiong, PEI Rong-fu, WANG Hao-lin, MEI Yan-xiong, WANG Yong-lei. Geological and geochemical characteristics of the Shizishan ore-field in Anhui Province [J]. *Rock and Mineral Analysis*, 2011, 30(4): 430–439. (in Chinese)
- [48] RITTMANN A. Note to contribution by V Gottini on the “serial character of the volcanic rock of Pantelleria” [J]. *Bull Volcanol*, 1970, 33: 979–981.
- [49] PEARCE J A. Trace element characteristics of lavas from destructive plate boundaries [M]. Chichester: John Wiley and Sons, 1982: 528–548.
- [50] PEARCE J A, HALTIS H B W, TINDELE A G. Trace element discrimination diagrams for the tectonic interpretation of granitic rocks [J]. *Journal of Petrology*, 1984, 25: 956–983.
- [51] PEARCE J A. Sources and settings of granitic rocks [J]. *Episodes*, 1996, 19: 120–125.
- [52] ZHOU Tao-fa, YUE Shu-cang, YUAN Feng, LIU Xiao-dong, ZHAO Yong. A discussion on petrological characteristics and genesis of Yueshan intrusion, Anhui Province [J]. *Geological Journal of China Universities*, 2001, 7(1): 70–80. (in Chinese)
- [53] LI Shu-guang. On the time of collision between the North China and Yangtze continental segments—The principle and application of isotope chronology [J]. *Geology of Anhui*, 1992, 2(4): 13–23. (in Chinese)
- [54] LIU Zhong-fa. Study on geological and geochemical characteristics and genesis of Dongguashan copper (gold) deposit, Tongling, Anhui Province [D]. Changsha: Central South University, 2014: 1–142. (in Chinese)

## 安徽铜陵冬瓜山矿床青山脚岩体的成岩机制

刘忠法<sup>1,2</sup>, 邵拥军<sup>1,2</sup>, 隗含涛<sup>1,2</sup>, 汪程<sup>1,2</sup>

1. 中南大学 有色金属成矿预测与地质环境监测教育部重点实验室, 长沙 410083;

2. 中南大学 地球科学与信息物理学院, 长沙 410083

**摘要:** 冬瓜山矿床是铜陵矿集区内一个大型的斑岩-矽卡岩型铜(金)多金属矿床, 矿区内的燕山期青山脚中酸性侵入岩体与成矿有直接的成因联系。在对青山脚岩体地质特征研究的基础上, 进行了详细的岩相学观察和系统的岩石化学、微量元素和稀土元素地球化学研究。分析了岩浆起源、成岩动力学环境及岩体的成岩作用过程, 并对青山脚岩体的成岩机制进行了探讨。结果表明, 青山脚岩体为高钾钙碱性岩石, 具有富集轻稀土元素、Th、Rb和Sr, 亏损重稀土元素、Ba、Nb和Ta的特征。形成成矿岩体的原始岩浆来源于地幔玄武质岩浆和地下壳部分熔融产生的正长岩岩浆的混合, 其成岩动力学环境为挤压到伸展的过渡环境。Harker图解和长石的混合结构表明, 岩浆在演化过程中发生了自身的分离结晶作用, 岩石化学及微量元素、稀土元素特征表明成岩过程中受到了地壳物质的混染。本区岩体是由壳幔混合岩浆在碰撞后的伸展环境中经过自身的分离结晶作用和与地壳的同化混染作用而形成的。

**关键词:** 青山脚岩体; 地质地球化学特征; 成岩动力学环境; 岩浆起源; 成岩作用; 冬瓜山铜(金)多金属矿床

(Edited by Wei-ping CHEN)